Prediction of Wide-Band Power Performance of MESFET Distributed Amplifiers Using the Volterra Series Representation

CHOI LOOK LAW AND COLIN S. AITCHISON

Abstract—**The power performance of a four-section MESFET distributed amplifier is predicted over the frequency range 2–8 GHz. The nonlinear model of the MESFET used has three nonlinear elements: g_m, g_d, and C_{gs}, which are represented by power series up to the third order. The analysis employs the Volterra series representation up to the third order. Experimental verification is first made on a 0.5×400-μm medium-power MESFET device to confirm the validity of the nonlinear model used in the analysis. The agreement between predicted and measured output power at 1-dB gain compression is within ±0.5 dBm across the 2–16 GHz band. A four-section distributed amplifier was then built with four 0.5×400-μm MESFET's. The agreement between predicted and measured output power at 1-dB gain compression of this amplifier is within ±0.7 dBm across the 2–8-GHz band. The measured output power at 1-dB gain compression is (22±1) dBm across the 2–8-GHz band.**

I. Introduction

VERY WIDEBAND solid-state GaAs MESFET amplifiers have been developed in the form of distributed amplifiers [1]. Most of these amplifiers are designed for low noise [2] and for operation in small-signal conditions [3]–[5]. There is a growing need to operate these amplifiers under large-signal conditions to give high output power. Kim *et al.* [6] have designed a distributed amplifier with 0.8-W output power at 1-dB gain compression. Their analysis, however, did not attempt to tune circuit elements for maximum output power. Such analysis requires a wide-band nonlinear model of the GaAs MESFET used and an efficient nonlinear analysis program.

Yamaguchi *et al.* [7] have made some effort to simulate the large-signal GaAs MESFET performance by numerical solution of the two-dimensional nonlinear differential equations describing the electron transport in the channel. The long computational time required to do this makes this approach impractical in circuit analysis and design programs. A device model was developed later by Willing *et al.* [8] using a quasi-static approach by measuring small-signal scattering parameters at a number of operating points to formulate an equivalent circuit, some of whose elements are bias-dependent. They then use polynomial forms to approximate these nonlinearities and a time-domain analysis program to calculate the large-signal device characteristics.

Peterson *et al.* [9] used the above method and extended their model to include effects of drain-to-gate breakdown currents and forward gate conduction. The circuit response was analyzed in the frequency domain and results were compared with those measured across the 8–18-GHz band. Measuring small-signal scattering parameters at many different operating points and then optimizing to get the equivalent circuit at these operating points make the above method rather laborious. Tajima *et al.* [10] used an alternative approach in the derivation of a nonlinear model. They postulate that the large-signal device properties are governed primarily by the transistor dc characteristics. This model was later extended to include drain-to-gate breakdown currents [11]. They then used the extended model to design a broad-band amplifier in the 7–18-GHz band.

This paper presents a wide-band nonlinear model of a MESFET in which the model elements are obtained easily by dc measurements, low-frequency measurements, and optimization of small-signal scattering parameters at one bias point. The three nonlinear elements considered are g_m, g_d, and C_{gs}; these are represented by power series up to the third order. The nonlinear analysis employed is that of the Volterra series representation up to the third order [12]. The validity of the model is confirmed by comparing measured and predicted output power at 1-dB gain compression of a 0.5×400-μm MESFET device across the 2–16-GHz band.

Also, the prediction of power performance of MESFET distributed amplifiers using the nonlinear MESFET model above, in conjunction with a highly efficient frequency-domain analysis, is presented for the first time. The nonlinear transfer functions [12] are computed using four-port chain matrix multiplications. The analysis is first checked by comparing the simulated power performance of distributed amplifiers having sections that vary in number from one to four with that simulated using SPICE2 [13]. A four-section distributed amplifier employing four 0.5×400-μm MESFET's is then built on Al_2O_3 substrate to verify the analysis experimentally.

Manuscript received March 29, 1986; revised June 26, 1986. This work was supported in part by the UK SERC.

C. L. Law is with the Department of Electronics and Electrical Engineering, King's College, London SW6 5PR, England.

C. S. Aitchison is with ERA Technology Ltd., Leatherhead, Surrey KT22 7SA, England.

IEEE Log Number 8610551.

0018-9480/86/1200-1308$01.00 ©1986 IEEE

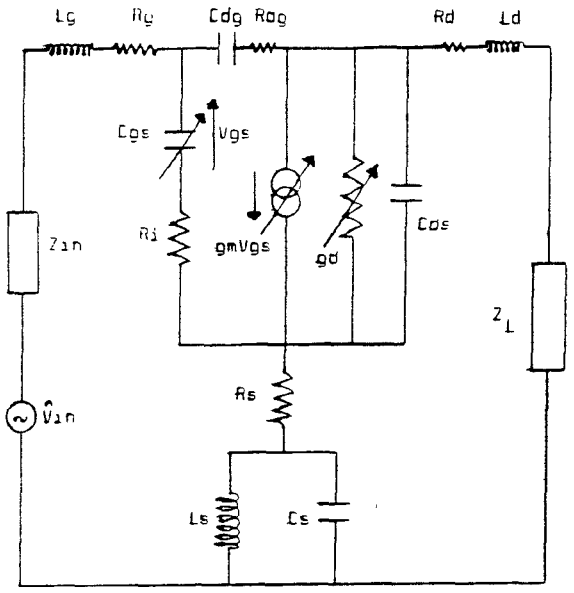

Fig. 1. MESFET nonlinear equivalent circuit.

II. MESFET Nonlinear Model and Nonlinear Analysis

The elements of the nonlinear equivalent circuit as shown in Fig. 1 can be divided into two types: linear elements and nonlinear elements. Values of these elements for a medium-power device biased at $V_{gs} = -1.0$ V and $V_{ds} =$ 8.0 V are tabulated in Table I. The linear elements are obtained by optimization of small-signal scattering parameters of the MESFET biased at its required operating point to give maximum output power.

The three nonlinear elements are g_m, g_d, and C_{gs}. Although g_m is a function of V_{gs} and V_{ds}, we restrict the nonlinearity of g_m to be a function of V_{gs} only for simplicity; it is expressed as

$$g_m = g_{m_0} + g_{m_1} V_{gs} + g_{m_2} V_{gs}^2. \tag{1}$$

This power series represents the instantaneous value of g_m when driven by an ac voltage V_{gs}, at the biased dc voltages V_{GS} and V_{DS}. The coefficients g_{m_0}, g_{m_1}, and g_{m_2} are found by a least-square polynomial curve-fitting routine to fit the slope of the measured dc curve I_{ds} versus V_{gs} at the biased V_{GS} and V_{DS}.

Similarly, g_d is a function of V_{gs} and V_{ds}. For simplicity, we restrict the nonlinearity of g_d to be a function of V_{ds} only; it is expressed as

$$g_d = g_{d_0} + g_{d_1} V_{ds} + g_{d_2} V_{ds}^2. \tag{2}$$

This power series represents the instantaneous value of g_d when driven by an ac voltage V_{ds} at the biased dc voltages V_{GS} and V_{DS}. Again, the coefficients g_{d_0}, g_{d_1}, and g_{d_2} are found using least-square polynomial curve-fitting routine to fit the measured curve of g_d versus V_{ds} at the biased V_{GS} and V_{DS}. The curve of g_d versus V_{ds} is measured with a 100-kHz signal using a technique similar to that employed by Mo and Yanai [14]. The 100-kHz signal is superimposed on the drain bias voltage and applied to the MESFET. The resultant ac voltage across the drain line is then measured. The drain is then substituted by a variable-resistance box. The conductance which gives the same ac voltage across it denotes the value of g_d at the biased V_{DS}. This bias voltage is varied and its corresponding value of g_d is measured to get the variation of g_d and V_{ds}. It should be noted that the amplitude of the 100-kHz signal applied should be as small as possible.

TABLE I
Values of the Nonlinear Model for a 0.5×400-μm MESFET

NE9000 V_{DS}=8.0v V_{GS}=-1.0v I_{DS}=50mA		
Lg= 0.46nH.	Cdg= 0.021pf.	gm=36.5+2.4Vgs-1.0Vgs^2(mS)
Rg= 0.5 ohm	Rdg= 29 ohm	
Ri= 5.4 ohm	Cds= 0.06pf.	gd=1.8-0.2Vds+0.02Vds^2(mS)
Rs= 2.0 ohm	Rd= 3.0 ohm	
Ls= 0.1 nH.	Ld= 0.5 nH.	Cgs=0.55+0.2Vgs+0.06Vgs^2 (pf.)
Cs= 0.15pf.		

The nonlinearity C_{gs} is approximated by the Schottky barrier diode capacitance between the gate and the source with V_{gs} as the sole voltage parameter. The least-square polynomial curve-fitting routine is used to fit the calculated values of C_{gs} from Schottky barrier theory into a power series of the form

$$C_{gs} = C_{gs_0} + C_{gs_1} V_{gs_1} + C_{gs_2} V_{gs}^2. \tag{3}$$

This power series represents the instantaneous value of C_{gs} when driven by an ac voltage V_{gs} at the biased dc voltages V_{GS} and V_{DS}.

The output $y(t)$ of a linear system can be related to its input $x(t)$ as

$$y(t) = \int_{-\infty}^{\infty} h(T) x(t-T) \tag{4}$$

where $h(T)$ is the transfer function of the system in the time domain. When the system becomes nonlinear, the output can be related to its input by the Volterra functional series

$$y(t) = \sum_{n=0}^{\infty} F_n(t) \tag{5}$$

where

$$F_n(t) = \int_{-\infty}^{\infty} \cdots \int_{-\infty}^{\infty} h_n(T_1, \cdots, T_n) x(t-T_1) \cdots x(t-T_n)\, dT_1 \cdots dT_n. \tag{6}$$

This series is convergent if a definite value of the functional corresponds to every function $x(t)$. This is true for the nonlinear system above since there is only one steady-state output $y(t)$ for a given input $x(t)$.

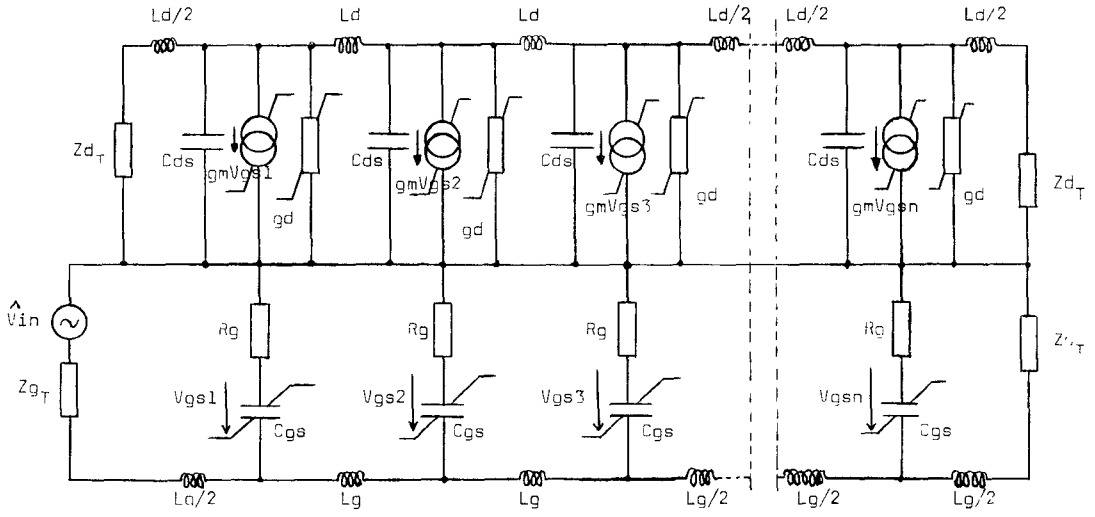

Fig. 2. Schematic diagram of an n-section distributed amplifier driven under large-signal condition.

For a system with mild nonlinearities, the output $y(t)$ can be related to its input $x(t)$ by the first three terms of the Volterra series [12] as

$$y(t) = \int_{-\infty}^{\infty} h_1(T)x(t-T)\,dT + \iint_{-\infty}^{\infty} h_2(T_1,T_2)x(t-T_1)x(t-T_2)\,dT_1\,dT_2 + \iiint_{-\infty}^{\infty} h_3(T_1,T_2,T_3)x(t-T_1)x(t-T_2)x(t-T_3)\cdot dT_1\,dT_2\,dT_3 + \cdots \quad (7)$$

where $h_1(T)$, $h_2(T_1,T_2)$, and $h_3(T_1,T_2,T_3)$ are the first-, second-, and third-order Volterra kernels, whose Fouriers transforms $H_1(W)$, $H_2(W_1,W_2)$, and $H_3(W_1,W_2,W_3)$ are their respective transfer functions in the frequency domain.

An efficient method of solving the transfer function of a system with power-series-type nonlinearity is the nonlinear current method described by Bussgang *et al.* [15]. Based on this method, the nonlinear transfer function $T_{NL}(W0)$ at the fundamental input frequency of the MESFET driven with one-tone input can be expressed as

$$T_{NL}(W0) = H_1(W0) + 3/4\hat{V}_{\text{in}}(W0)\hat{V}_{\text{in}}(-W0)H_3(W0,W0,-W0) + \cdots \quad (8)$$

where the available power of the source can be expressed as

$$P_{\text{av}}(W0) = \hat{V}_{\text{in}}^2(W0)/8\,\text{Re}\left[Z_{\text{in}}(W0)\right]. \quad (9)$$

From (8) and (9), the transducer gain of the MESFET embedded between 50 Ω at the input and output can be expressed as

$$G_T(W0) = 4|H_1(W0) + 6P_{\text{av}}(W0)\,\text{Re}(Z_{\text{in}})H_3(W0,W0,-W0)|^2 + \cdots. \quad (10)$$

From (10), we can see that the gain is made up of two parts. The first is a linear function, $H_1(W0)$. The second part is proportional to the third-order nonlinear transfer function $H_3(W0,W0,-W0)$ and it increases with increasing available input power. $\text{Re}[H_3(W0,W0,-W0)]$ usually have opposite signs to $\text{Re}[H_2(W0)]$, thus resulting in gain compression as the available input power increases. This theory applies until the real part of the transfer function $T_{NL}(W0)$ becomes negative. From (8) and (9), that can be expressed in the inequality

$$\frac{\text{Re}\left[\dfrac{H_1(W0)}{H_3(W0,W0,-W0)}\right]}{6\,\text{Re}(Z_{\text{in}})} \geq P_{\text{av}}(W0) \geq 0. \quad (11)$$

This inequality defines the range of available input power to the system in which the power gain expression in (10) holds.

III. Distributed Amplifier Nonlinear Analysis Using Volterra Series

Fig. 2 shows an n-section distributed amplifier with the MESFET's represented by a unilateral nonlinear model. When the input and output signals are small, the amplifier is said to be operating in the linear region. From (1)–(3), the nonlinear elements in the MESFET's reduce to their first-order coefficients g_{m_0}, g_{d_0} and C_{gs_0}. The linear transfer function can be easily found by four-port transmission matrix multiplications. As the input signal increases, the instantaneous values of g_m, g_d, and C_{gs} change with the level of the input signal. The amplifier is now said to be operating into its nonlinear region. Provided the nonlinearities are mild, the output of this amplifier can be represented by the Volterra series up to the third order [12], as in (7). The Fourier transform of the Volterra kernels gives their respective nonlinear transfer functions in the frequency domain. Using the nonlinear current method [15], the second-order nonlinear transfer function $H_{2L}(W1,W2)$ can be found by replacing the nonlinear elements by their respective second-order nonlinear currents across them. If the nonlinearity C_{gs} is negligible (i.e., its effect is small compared to g_m and g_d), we can neglect

the interactions between the second-order gate voltages of all the MESFET's. By applying the theory of superposition

$$H_{2L}(W1, W2) = \sum_{i=1}^{n} H_{2Li}(W1, W2) \qquad (12)$$

where $H_{2Li}(W1, W2)$ is the second-order nonlinear transfer function with the ith MESFET being nonlinear while the rest are all linear. $H_{2Li}(W1, W2)$ is solved by first solving for the currents in the ith MESFET. Referring to Fig. 3, this can be done by solving the following matrix

$$\begin{bmatrix} H_{12}(W') \\ H_{22}(W') \\ H_{32}(W') \end{bmatrix} = \begin{bmatrix} Z11 & Z12 & Z13 \\ Z21 & Z22 & Z23 \\ Z31 & Z32 & Z33 \end{bmatrix} \begin{bmatrix} I11 \\ I21 \\ I31 \end{bmatrix}$$

where

$$\begin{aligned}
W' &= W1 + W2 \\
Z11 &= Z_{\text{in}}(W') + Z_g(W') + Z_s(w') \\
Z12 &= -Z_g(W') \\
Z13 &= -Z_s(W') \\
Z21 &= -\left[Z_g(W') + g_{m_0} Z_{ds}(W')/jW'C_{gs_0}\right] \\
Z22 &= Z_g(W') + Z_{ds}(W') + Z_{dg}(W') \\
&\quad + g_{m_0} Z_{ds}(W')/jW'C_{gs_0} \\
Z23 &= -Z_{ds}(W'), \\
Z31 &= -\left[Z_s(W') - g_{m_0} Z_{ds}(W')/jW'C_{gs_0}\right] \\
Z32 &= \left[Z_{ds}(W') + g_{m_0} Z_{ds}(W')/jW'C_{gs_0}\right] \\
Z33 &= Z_{ds}(W') + Z_l(W') + Z_s(W') \\
H_{12}(W') &= I2c_g/jW'C_{gs_0} \\
H_{22}(W') &= [I2g_m + I2g_d] Z_{ds}(W') \\
&\quad - H_{12}(W')\left[1 + g_{m_0} Z_{ds}(W')\right] \\
H_{32}(W') &= -\left[H_{22}(W') + H_{12}(W')\right] \\
I2c_g &= jW'C_{gs_1} H_{1C}(W1) H_{1C}(W2) \\
I2g_m &= g_{m_1} H_{1C}(W1) H_{1C}(W2) \\
I2g_d &= g_{d_1} H_{1D}(W1) H_{1D}(W2).
\end{aligned}$$

$Z_{\text{in}}(W')$ and $Z_l(W')$ are the input and output impedances seen by the nonlinear MESFET considered. These impedances are therefore related to the characteristic impedances at the gate and drain line of the distributed amplifier. They are found by transforming the transmission matrix of a Z matrix. This transformation, together with some essential elements in four-port transmission matrices, is presented in the Appendix. Similarly, $H_{3L}(W1, W2, W3)$ can be found by replacing the nonlinear elements by their respective third-order nonlinear currents. By going through the same procedure as in the derivation of second-order nonlinear transfer function, $H_{3L}(W1, W2, W3)$ can be expressed as

$$H_{3L}(W1, W2, W3) = \sum_{i=1}^{n} H_{3Li}(W1, W2, W3). \qquad (13)$$

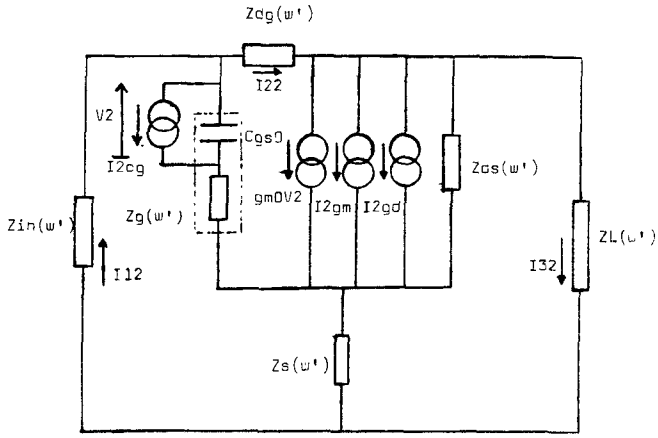

Fig. 3. Schematic diagram of a MESFET driven by second-order nonlinear currents.

$H_{3Li}(W1, W2, W3)$ is solved by solving the matrix (Fig. 4)

$$\begin{bmatrix} H_{13}(W'') \\ H_{23}(W'') \\ H_{33}(W'') \end{bmatrix} = \begin{bmatrix} Z11 & Z12 & Z13 \\ Z21 & Z22 & Z23 \\ Z31 & Z32 & Z33 \end{bmatrix} \begin{bmatrix} I13 \\ I23 \\ I33 \end{bmatrix}$$

where

$$\begin{aligned}
W'' &= W1 + W2 + W3 \\
Z11 &= Z_{\text{in}}(W'') + Z_g(W'') + Z_s(W'') \\
Z12 &= -Z_g(W'') \\
Z13 &= -Z_s(W'') \\
Z21 &= -\left[Z_g(W'') + g_{m_0} Z_{ds}(W'')/jW''C_{gs_0}\right] \\
Z22 &= Z_g(W'') + Z_{ds}(W'') + Z_{dg}(W'') \\
&\quad + g_{m_0} Z_{ds}(W'')/jW''C_{gs_0} \\
Z32 &= -Z_{ds}(W'') \\
Z31 &= -\left[Z_s(W'') - g_{m_0} Z_{ds}(W'')/jW''C_{gs_0}\right] \\
Z32 &= -\left[Z_{ds}(W'') + g_{m_0} Z_{ds}(W'')/jW''C_{gs_0}\right] \\
Z33 &= Z_{ds}(W'') + Z_l(W'') + Z_s(W'') \\
H_{13}(W'') &= I3c_g/jW''C_{gs_0} \\
H_{23}(W'') &= Z_{ds}(W'')[I3g_m + I3g_d] \\
&\quad - H_{13}(W'')\left[1 + g_{m_0} Z_{ds}(W'')\right] \\
H_{33}(W'') &= -\left[H_{23}(W'') + H_{13}(W'')\right] \\
I3c_g &= jW''C_{gs_2} H_{1C}(W1) H_{1C}(W2) H_{1C}(W3) \\
&\quad + 2jW''C_{gs_1} \overline{H_{1C}(W1) H_{2C}(W2, W3)} \\
I3g_m &= g_{m_2} H_{1C}(W1) H_{1C}(W2) H_{1C}(W3) \\
&\quad + 2_{gm_1} \overline{H_{1C}(W1) H_{2C}(W2, W3)} \\
I3g_d &= g_{d_2} H_{1D}(W1) H_{1D}(W2) H_{1D}(W3) \\
&\quad + 2g_{d_1} \overline{H_{1D}(W1) H_{2D}(W2, W3)}
\end{aligned}$$

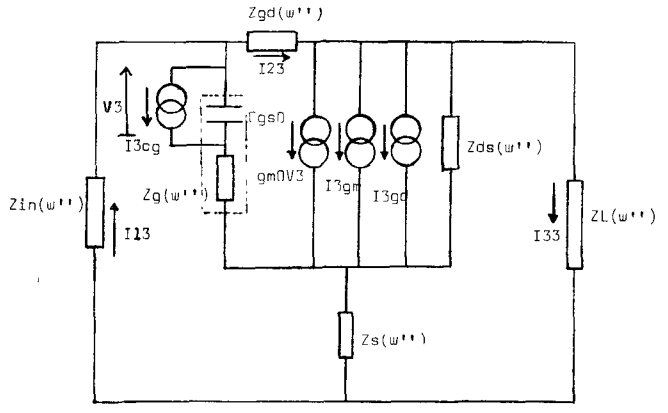

Fig. 4. Schematic diagram of a MESFET driven by third-order nonlinear currents.

where the overhead bar indicates symmetrization. We can now summarize the whole process of determining the nonlinear transfer function $T_{NA}(W0)$ of the n-section distributed amplifier with one tone input by the following flow chart:

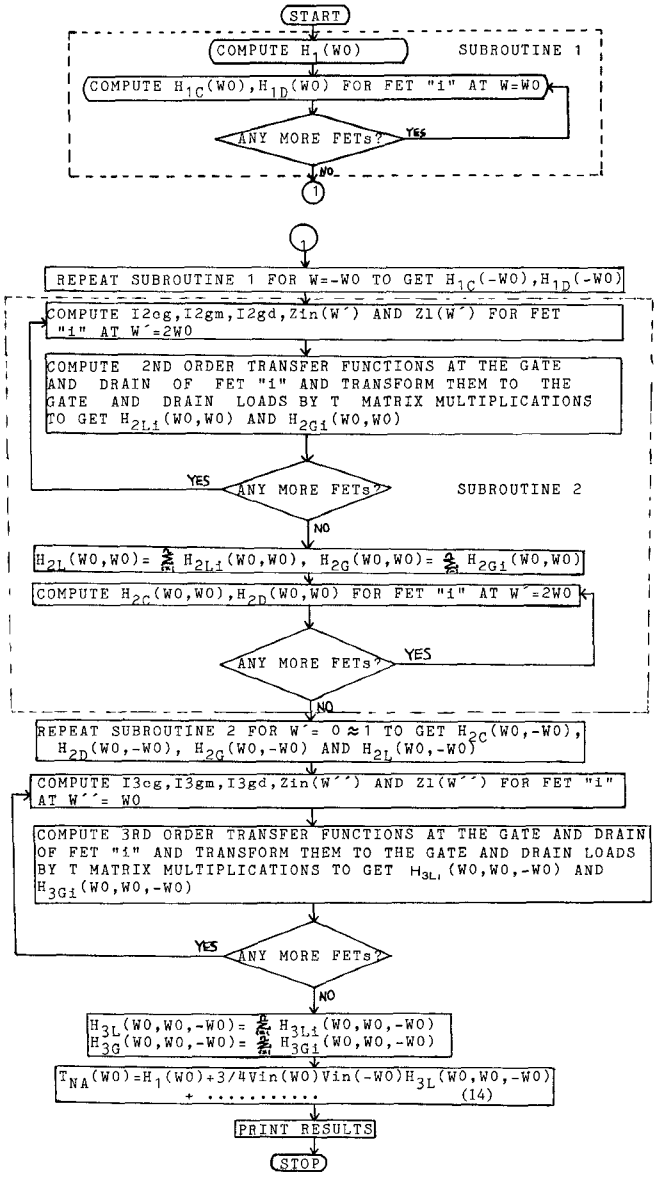

The voltage across the output load of the amplifier at the fundamental input frequency is given by

$$V_{OL}(W0) = T_{NA}(W0)V_{\text{in}}(W0). \tag{15}$$

The power dissipated across the load due to $V_{OL}(W0)$ is

$$P_{\text{OUT}}(W0) = |V_{OL}(W0)|^2 \,\text{Re}\,[Z1(W0)]/|Z1(W0)|^2. \tag{16}$$

The available input power from the source is given by (9). The transducer gain of the amplifier can thus be expressed as

$$G_{TA}(W0) = 4\,\text{Re}\,[Z_s(W0)]\,\text{Re}\,[Z_l(W0)]/ \left[|Z_l(W0)|^2\right]|H_1(W0) + 6P_{\text{av}}(W0) \cdot \text{Re}\,[Z_s(W0)]\,H_3(W0, W0, -W0)|^2 + \cdots. \tag{17}$$

$\text{Re}[H_3(\text{W0},\text{W0},-\text{W0})]$ usually has signs opposite the $\text{Re}[H_1(W0)]$, resulting in gain compression as the available input power increases. The range of available input power to which this theory applies is given above by inequality (11). The output power of an amplifier is usually quoted at 1-dB gain compression. From (16), the corresponding available input power $P_{\text{av1dB}}(W0)$, can be expressed in dBm as

$$P_{\text{av1dB}}(W0) = 12.6 - 10\log_{10}[-\text{Re}\,[Z_s(W0)] \cdot \text{Re}\,[H_3(W0, W0, -W0)/H_1(W0)]]. \tag{18}$$

Since $P_{\text{out}}(W0) = G_{TA}(W0)P_{\text{av}}(W0)$, the output power 1-dB gain compression can be expressed as

$$P_{\text{out1dB}}(W0) = 10\log_{10}\{4\,\text{Re}\,[Z_s(W0)]\,\text{Re}\,[Z_l(W0)] \cdot |H_1(W0)^2/|Z_l(W0)|^2\} - 10\log_{10}\{-\text{Re}\,[Z_s(W0)]\,\text{Re}\,[H_3(W0, W0, -W0)/H_1(W0)]\} + 11.6 \cdots. \tag{19}$$

We can see that the output power at 1-dB gain compression is dependent on the functions $H_1(W0)$ and $H_3(W0, W0, -W0)$ and on load and source impedances. Note that the second term has a negative sign inside the $\log_{10}$ function. This is multiplied by the negative sign resulting from $\text{Re}[H_3(W0, W0, -W0)/H_1(W0)]$ to give a positive value. The nonlinear analysis is incorporated into a computer program names LSDAR.

IV. Experimental Verifications and Discussions

This consists of three parts. This first is to verify the validity of the nonlinear model across the 2–16-GHz band by comparing predicted and measured transducer gain, versus available input power at a number of chosen frequencies across that band. The second part verifies the validity of the distributed amplifier nonlinear analysis using the Volterra series up to the third order, across the 2–8-GHz band. This is done by comparing the simulated power performance of one-, two-, and four-section distrib-

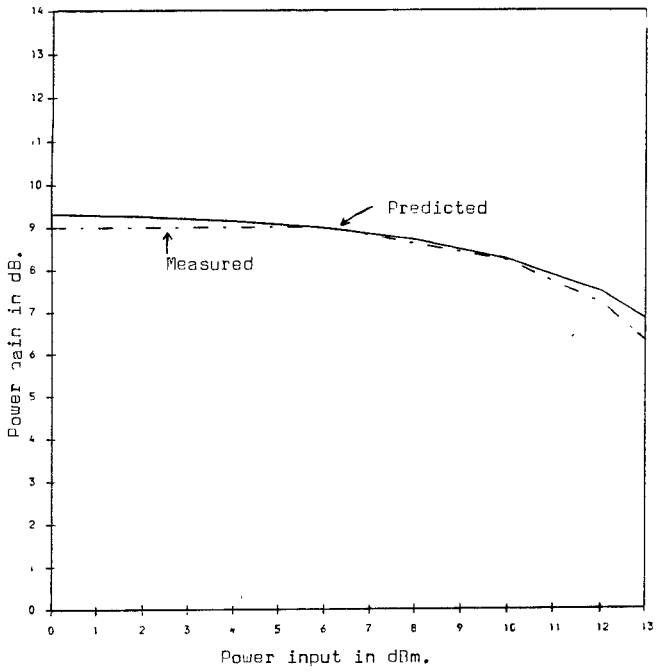

Fig. 5. Predicted and measured power gain versus available input power for a 0.5×400-μm MESFET at 2 GHz.

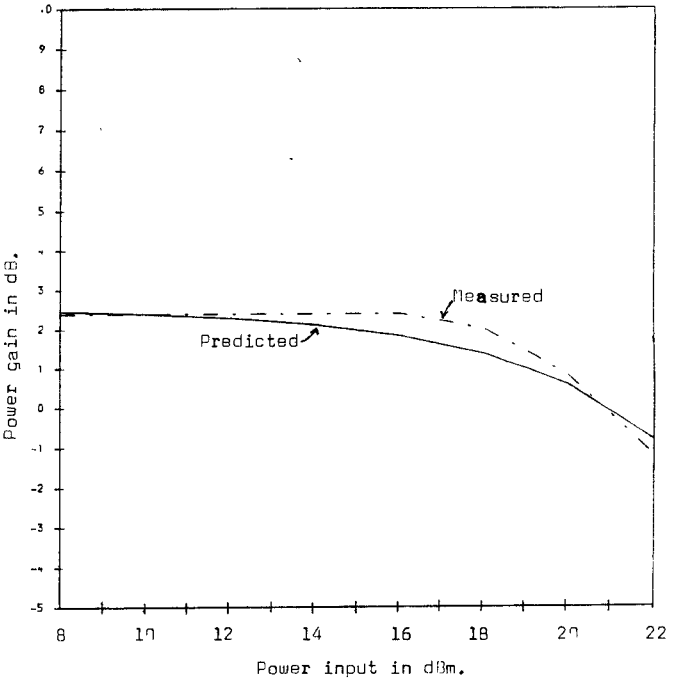

Fig. 7. Predicted and measured power gain versus available input power for a 0.5×400-μm MESFET at 12 GHz.

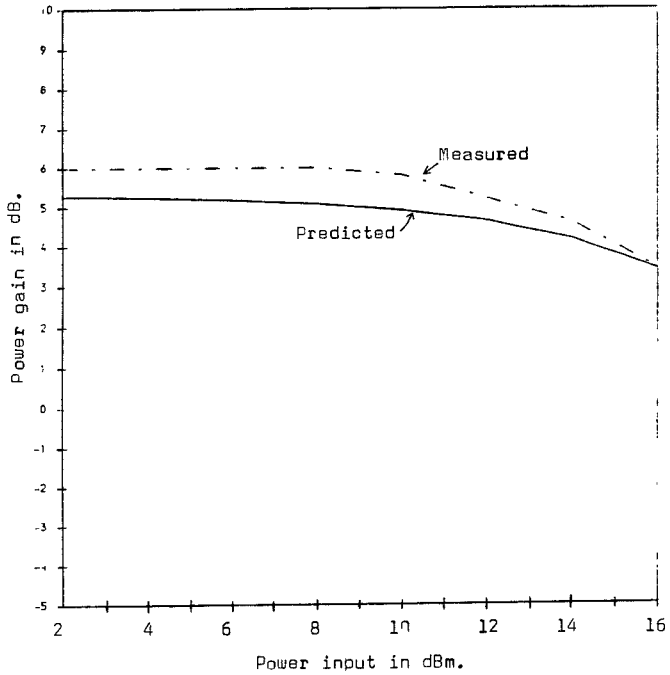

Fig. 6. Predicted and measured power gain versus available input power for a 0.5×400-μm MESFET at 8 GHz.

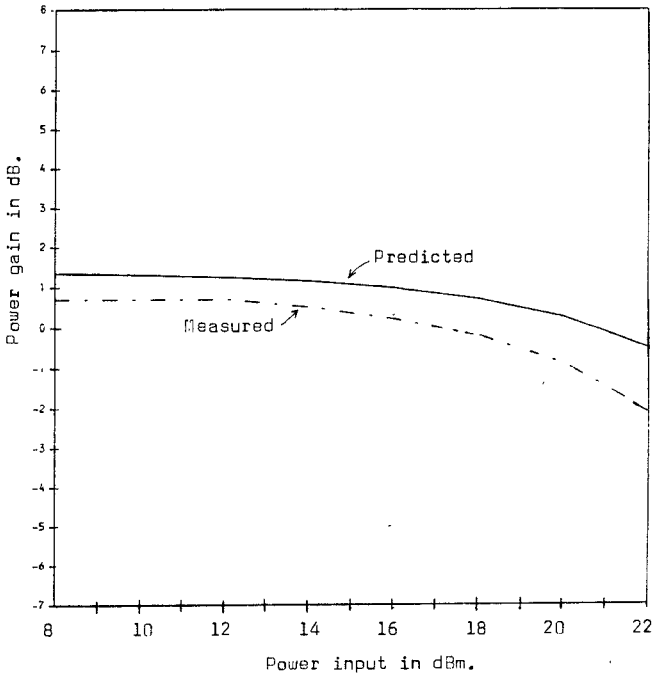

Fig. 8. Predicted and measured power gain versus available input power for a 0.5×400-μm MESFET at 14 GHz.

uted amplifiers at a number of frequencies with those simulated by SPICE2. The third part examines the predicted and measured output power at 1-dB gain compression for a four-section distributed amplifier employing four 0.5×400-μm MESFET's.

A. Verification of Nonlinear Model

A 0.5×400-μm NEC MESFET was embedded between 50-Ω input and output microstrip lines built on 1-in-square alumina substrate. The device nonlinear model was first found using the method described earlier in this work, and the values of the elements are shown in Table I. The power performance of the MESFET was predicted and measured using the setup shown in Fig. 15 across the 2–16-GHz band. The validity of the nonlinear model was checked by plotting the transducer gain versus available input power at a number of frequencies (Figs. 5–8). The agreement of

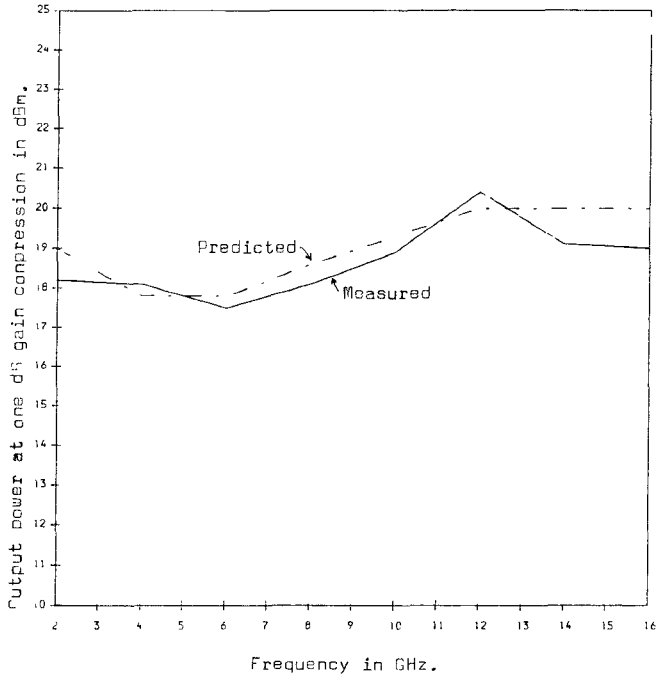

Fig. 9. Predicted and measured output power at 1-dB gain compression for a 0.5×400-μm MESFET.

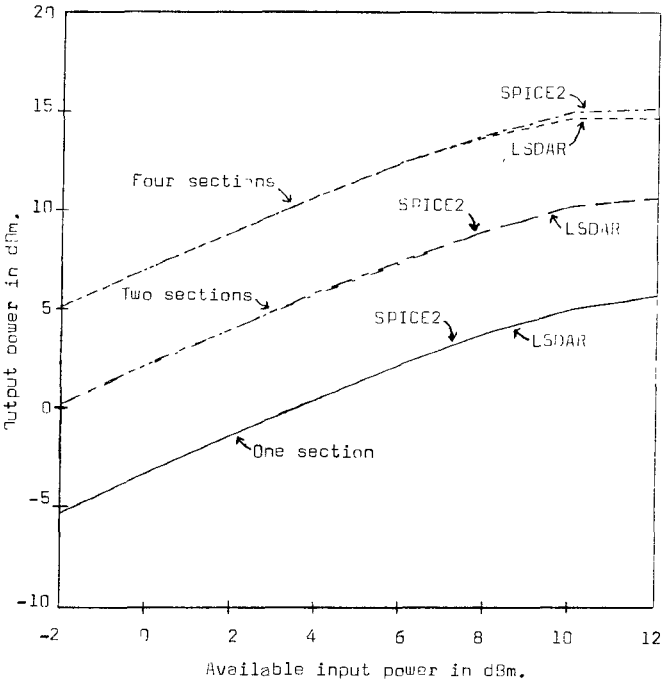

Fig. 11. Simulated power performance of distributed amplifiers with one, two, and four sections of 4 GHz.

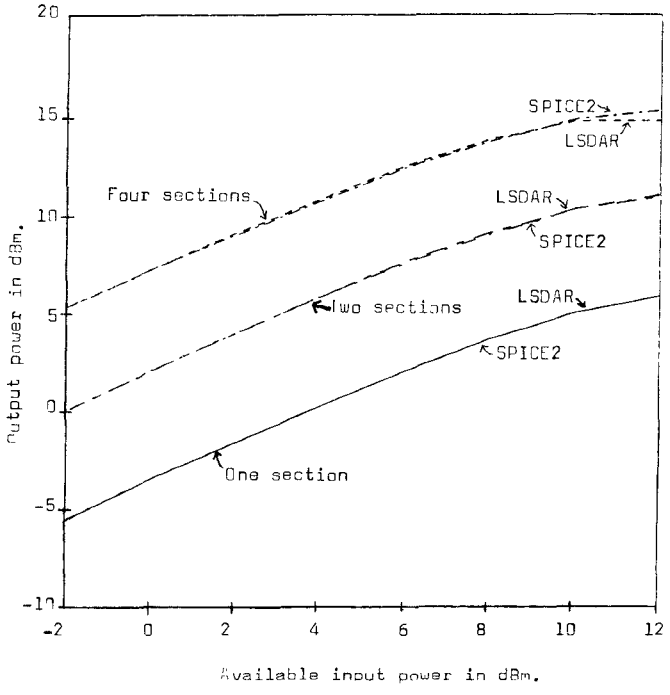

Fig. 10. Simulated power performance of distributed amplifiers with one, two, and four sections at 2 GHz.

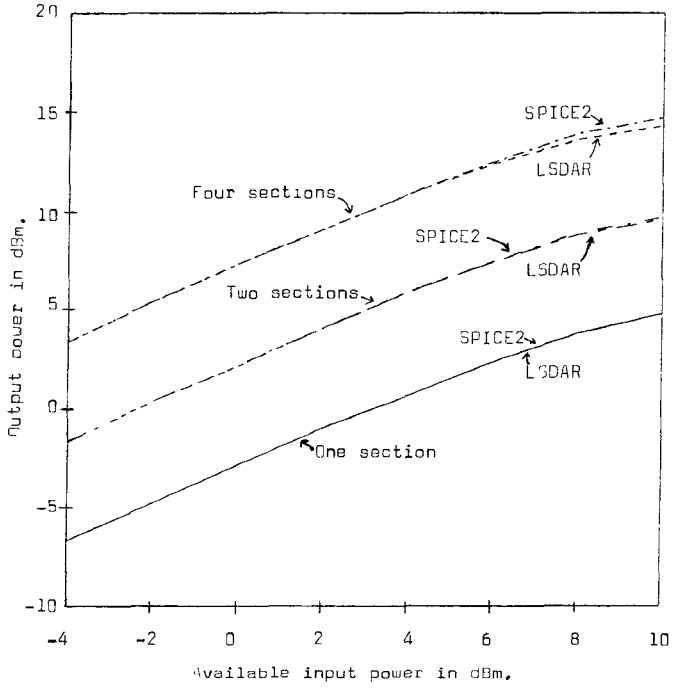

Fig. 12. Simulated power performance of distributed amplifiers with one, two, and four sections at 6 GHz.

1-dB gain compression between the predicted and measured output power was within ± 0.5 dBm (Fig. 9).

B. Comparison Between Simulated Power Performance of Distributed Amplifiers using LSDAR and SPICE2

The power performances of one-, two-, and four-section distributed amplifiers were simulated using the nonlinear analysis program LSDAR described in this work at various frequencies across the 2–8-GHz band. The results were compared with those simulated using SPICE2. The values of the nonlinear elements, corresponding to a 0.5×200-μm MESFET, used for the simulations were

$$C_{gs} = 0.21 + 0.45V_{gs} \quad \text{(pF)}$$

$$g_m = 37.0 + 12.5V_{gs} - 4.2V_{gs}^2 \quad \text{(mS)}$$

$$g_d = 2.43 - 0.63V_{ds} + 0.03V_{ds}^2 \quad \text{(mS)}.$$

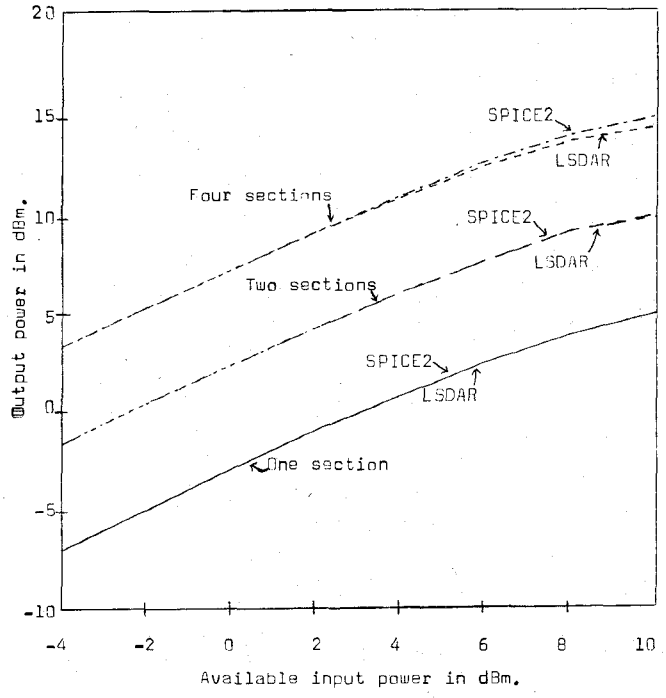

Fig. 13. Simulated power performance of distributed amplifiers with one, two, and four sections at 8 GHz.

The agreement between the simulated power using LSDAR and SPICE2 (Figs. 10–13) was very good. It should be noted that SPICE2 is a time-domain analysis program requiring around 30 min CPU time on the Harris 500 minicomputer to compute the output power for a four-section distributed amplifier with 10-dBm available input power at 8 GHz. The program LSDAR, in comparison, gives the full power performance across the 2–8-GHz band in less than 2 min on the same computer.

C. Comparison Between Predicted and Measured Output Power at 1-dB Gain Compression

A four-section distributed amplifier employing four 0.5 $\times$400-μm MESFET devices was built on 1-in-square alumina substrate using the lumped components technique [16]. A photograph of the amplifier is shown in Fig. 14. All the inductors were realized using 25-μm-diameter bond wires. Padding capacitors in the form of open-end microstrip lines were distributed along the drain line to enable the signals propagating down the gate line to be in phase with those in the drain. The power performance of this amplifier was measured across the 2–8-GHz band using the setup shown in Fig. 15. The predicted and measured output power at 1-dB gain compression (Fig. 16) is (22 ± 1) dBm with small-signal power gain of (5 ± 2) dB. The agreement between the predicted and measured results is within ± 0.7 dBm.

Simulations have been made on distributed amplifiers beyond 8 GHz using the program LSDAR. It has been found that the theory cannot model the gain compression properly, especially when the amplifier has more than two sections. In some cases, gain expansion is observed. This is believed to be caused by the fact that we have neglected the effects of interactions between second- and third-order gate voltages of the MESFET's. These interactions can be significant at higher frequencies because of the feedback from drain to gate. Also, we have only considered three terms in the Volterra series expansion. Analysis using SPICE2 in such cases shows that the fourth and fifth harmonic output components are significant. Work is underway at the moment to include these interactions between MESFET's at the gate and also to expand the analysis up to the fifth order.

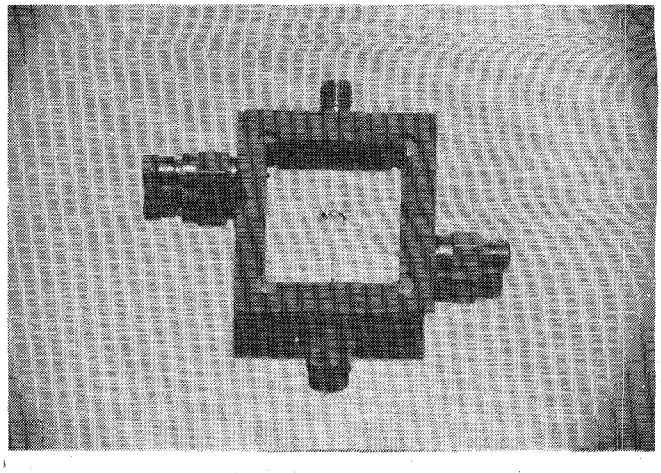

Fig. 14. Photograph of the four-section distributed amplifier.

V. Conclusions

A wide-band nonlinear model for GaAs MESFET devices is demonstrated to be valid up to 16 GHz. The frequency-domain nonlinear analysis based on the Volterra series representation up to the third order can predict 1-dB gain compression of distributed amplifiers across the 2–8-GHz band. By simulating the power performance with one nonlinear element at a time, the major cause of gain compression can be identified. Expressions for the nonlinear transfer functions of a distributed amplifier can be derived in terms of its circuit parameters using the analysis presented in this work. The design of distributed amplifiers can then be optimized for maximum output power at the 1-dB gain compression. This analysis can also be easily modified to predict third-order intermodulation.

Appendix

Four-port transmission matrix for impedances:

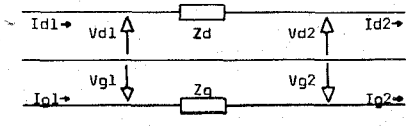

$$\begin{bmatrix} V_{d1} \\ I_{d1} \\ V_{g1} \\ I_{g1} \end{bmatrix} = \begin{bmatrix} 1 & Z_d & 0 & 0 \\ 0 & 1 & 0 & 0 \\ 0 & 0 & 1 & Z_g \\ 1 & 0 & 0 & 1 \end{bmatrix} \begin{bmatrix} V_{d2} \\ I_{d2} \\ V_{g2} \\ I_{g2} \end{bmatrix}.$$

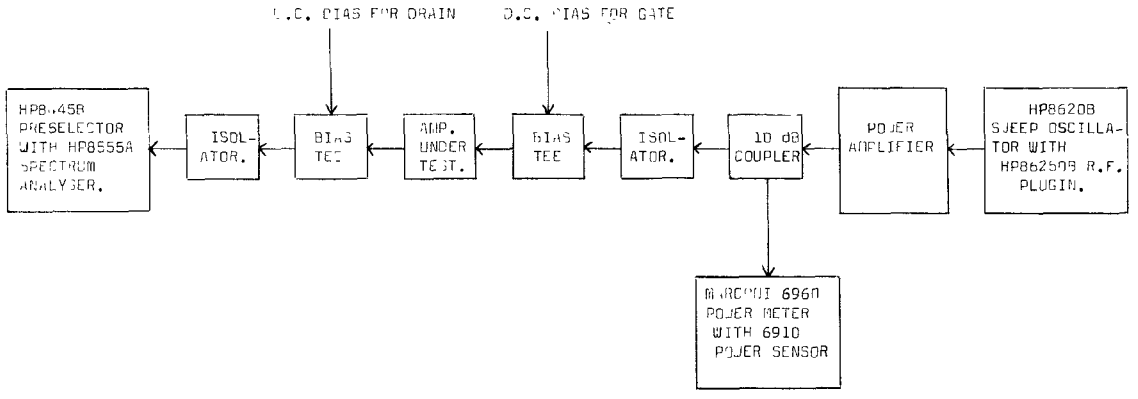

Fig. 15. Experimental setup for measuring power performance.

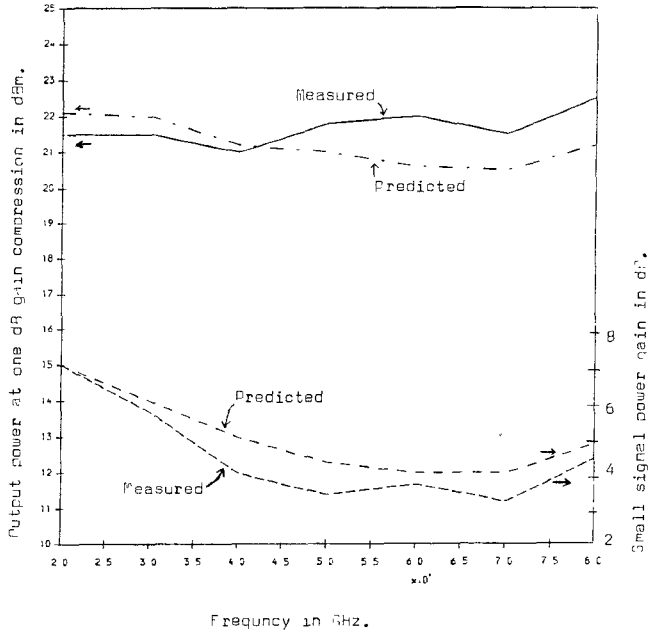

Fig. 16. Predicted and measured output power at 1-dB gain compression together with small-signal power gain for a four-section distributed amplifier. Results are predicted with $g_m = 36.5 + 1.9V_{gs} - 2.1V_{gs}^2$ (mS) and $g_d = 1.8 - 0.35V_{ds} + 0.05V_{ds}^2$ (mS).

Four-port transmission matrix for MESFET in terms of its two-ports Y parameters.

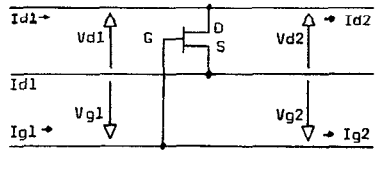

$$\begin{bmatrix} V_{d1} \\ I_{d1} \\ V_{g1} \\ I_{g1} \end{bmatrix} \begin{bmatrix} 1 & \cdot & 0 & \cdot & 0 & \cdot & 0 \\ Y22 & \cdot & 1 & \cdot & Y21 & \cdot & 0 \\ 0 & \cdot & 0 & \cdot & 1 & \cdot & 0 \\ Y12 & \cdot & 0 & \cdot & Y11 & \cdot & 1 \end{bmatrix} \begin{bmatrix} V_{d2} \\ I_{d2} \\ V_{g2} \\ I_{g2} \end{bmatrix}.$$

Transformation from T matrix to Z matrix.

$$Z11 = (T11T43 - T13T41)/(T21T43 - T23T41)$$
$$Z12 = (T11T23 - T21T13)/(T41T23 - T21T43)$$
$$Z21 = (T33T41 - T31T43)/(T23T41 - T21T43)$$
$$Z22 = (T21T33 - T31T23)/(T43T21 - T41T23)$$
$$Z31 = T43/(T21T43 - T23T41)$$
$$Z32 = T23/(T41T23 - T43T21)$$
$$Z41 = T41/(T23T41 - T21T43)$$
$$Z42 = T21/(T43T21 - T41T23).$$

The K symbol below indicates the inverse of the T matrix:

$$Z13 = K43/(K21K43 - K23K41)$$
$$Z14 = K23/(K41K23 - K43K21)$$
$$Z23 = K41/(K23K41 - K21K41)$$
$$Z24 = K21/(K43K21 - K41K23)$$
$$Z33 = (K11K43 - K13K41)/(K21K43 - K23K41)$$
$$Z34 = (K11K23 - K21K13)/(K41K23 - K21K43)$$
$$Z43 = (K33K41 - K31K43)/(K23K41 - K21K43)$$
$$Z44 = (K33K21 - K31K23)/(K43K21 - K41K23).$$

ACKNOWLEDGMENT

The authors wish to thank O. S. A. Tang and C. Camacho-Penalosa for their helpful discussions.

REFERENCES

[1] E. L. Ginzton, W. R. Hewlett, J. W. Jasberg, and J. D. Noe, "Distributed amplifications," *Proc. IRE*, vol. 36, pp. 956–969, 1948.

[2] C. S. Aitchison, "The intrinsic noise figure of the MESFET distributed amplifier," *IEEE Trans. Microwave Theory Tech.*, vol MTT-33, June 1985.

[3] Y. Ayasli, L. D. Reynolds, J. L. Vorhaus, and L. K. Hanes, "2–20 GHz GaAs travelling-wave amplifiers," *IEEE Trans. Microwave Theory Tech.*, vol. MTT-32, pp. 71–77, 1984.

[4] W. Kennan, T. Andrade, and C. Huang, "A miniature 2–18 GHz monolithic GaAs distributed amplifier," in *IEEE Microwave and Millimeter-Wave Monolithic Circuits Symp. Dig.* (San Francisco), 1984, pp. 41–44.

[5] C. L. Law and C. S. Aitchison, "2–18 GHz distributed amplifier in hybrid form," *IEE Electronic Lett.*, vol. 21, no. 16, pp. 684–685, Aug. 1985.
[6] B. Kim, H. Q. Tsang, and H. D. Shih, "High power distributed amplifier using MBE synthesized material," in *IEEE Microwave and Millimeter-Wave Monolithic Circuits Symp. Dig.* (St. Louis), 1985, pp. 35–37.
[7] K. Yamaguchi, S. Asai, and K. Kodera, "Two-dimensional numerical analysis of stability criteria of GaAs FETs," *IEEE Trans. Electron Devices*, vol. ED-23, pp. 1283–1290, Dec. 1976.
[8] H. A. Willing, C. Rauscher, and P. de Santis, "A technique for predicting large-signal performance of a GaAs MESFET," *IEEE Trans. Microwave Theory Tech.*, vol. MTT-26, pp. 1017–1023, Dec. 1978.
[9] D. L. Peterson, A. M. Pavio, and B. Kim, "A GaAs FET model for large-signal applications," *IEEE Trans. Microwave Theory Tech.*, vol. MTT-32, pp. 276–281, Mar. 1984.
[10] Y. Tajima, B. Wrona, and K. Mishima, "GaAs FET large-signal model and its application to circuit designs," *IEEE Trans. Electron Devices*, vol. ED-28, pp. 171–175, Feb. 1981.
[11] Y. Tajima and P. D. Miller, "Design of broad-band power GaAs FET amplifiers," *IEEE Trans. Microwave Theory Tech.*, vol. MTT-32, pp. 261–267, Mar. 1984.
[12] N. Wiener, "Response of a nonlinear device to noise," MIT Radiation Lab., Rep. V-16S, April 6, 1942.
[13] L. W. Nagel, "SPICE2: A computer program to simulate semiconductor circuits," Electronics Res. Lab., Univ. of California, Berkeley, Mem. EPL-M520, May 9, 1975.
[14] D. L. Mo and H. Yanai, "Current–voltage characteristics of the junction-gate field-effect transistor with field dependent mobility," *IEEE Trans. Electron Device*, vol., ED-17, pp. 577–586, 1970.
[15] J. Bussgang, L. Ehrman, and J. Graham, "Analysis of nonlinear systems with multiple inputs," *Proc. IEEE*, vol. 62, pp. 1089–1119, Aug. 1974.
[16] C. S. Aitchison *et al.*, "Lumped-circuit elements at microwave frequencies," *IEEE Trans. Microwave Theory Tech.*, vol. MTT–19, Dec. 1971.

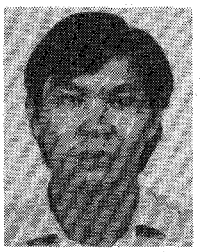

Choi Look Law was born in Sarawak, Malaysia, in August 1961. He received the B.Sc. degree in electronics engineering from Chelsea College, London University, in 1983. He joined the active microwave research group in the same college in 1984 as a research assistant, working in the area of distributed amplifiers. The project, supported by SERC, was to investigate the power performance of distributed amplifiers. He is also working towards the Ph.D. degree in this area.

He will soon be joining the microwave research and development group in ERA Technology Ltd. at Leatherhead, Surrey, England. His interests are in microwave power amplifiers and mixers.

✠

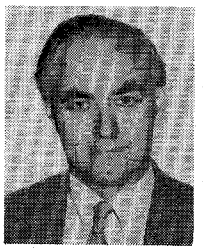

Colin S. Aitchison was born in Morecambe, England, in 1933. He received the B.Sc. and A.R.C.S. degrees in physics from Imperial College, London University, London, England, in 1955.

He worked for Philips Research Laboratories, Redhill, Surrey, England, from 1955 to 1972, being initially concerned with the noise-reduction properties of direct injection phase-locked klystrons for use with Doppler radars. He led a group concerned with parametric amplifiers, mixers, ferrite limiters, lumped microwave components, and Gunn and avalanche oscillators. In 1972, he joined the Department of Electronics, Chelsea College, University of London, where he was Professor of Electronics. He has recently joined ERA Technology Ltd. at Leatherhead, Surrey, England. His research interests remain in the field of active microwave circuits, particularly distributed amplifiers.

Professor Aitchison is a Fellow of the Institute of Electrical Engineers, a member of the Institute of Physics, and an Emeritus Professor of the University of London.